SATURATION CHARACTERISTICS OF COUNTERSTREAMING WARM ELECTRONS

by

A. Wendt

Memorandum No. UCB/ERL M85/45

28 May 1985

ELECTRONICS RESEARCH LABORATORY

College of Engineering
University of California, Berkeley
94720

Saturation Characteristics of Counterstreaming Warm Electrons

Department of Electrical Engineering and Computer Science
and the Electronics Research Laboratory
University of California
Berkeley, CA 94720

Abstract

An investigation has been made of the electron-electron two stream instability as the beam temperatures were increased, using particle simulations. Growth rates and saturation characteristics were studied and compared to theoretical models. The final state of the system, characterized by the value of the distribution function at zero velocity, $f(v = 0)$, was found to evolve to a Maxwellian in the cold case, and to a double-peaked distribution stable by the Penrose criterion in the warm case.

Amy Wendt (Prof. C. K. Birdsall)
May 3, 1985

Introduction

Kainer, et. al. [1] observed a transition in the character of the beam plasma instability as the density of the beam was varied relative to that of the plasma. Our study examines the changes in the electron-electron two stream instability as the beam temperatures are increased, in search of a similar transition. $ES1$, a particle simulation computer code, was run with beam temperatures varying from zero to so warm that no instability occurred. In particular, the program was used to study the growth rates of unstable modes and observe the time evolution of the velocity distribution. The simulation results were compared with theoretical growth rates and stability condiions. No well-defined transition as observed for the beam-plasma instability was found.

Theory

The theoretical growth rates of the various modes of the two stream instability are given by the dispersion relation $D(\omega, k) = 0$. This relation can be found by solving [2]

$$1 = \frac{\omega_p^2}{k^2} \frac{\partial}{\partial \xi} \int \frac{F(v)dv}{v - \xi}, \tag{1}$$

where

$$\xi = \frac{\omega}{k}$$

and ω_p is the plasma frequency, defined by

$$\omega_p^2 = \frac{ne^2}{m},$$

and $F(v)$ is the velocity distribution function normalized to

$$\int F(v)dv = 1.$$

For the two stream distribution,

$$F(v) = \frac{1}{2v_t\sqrt{2\pi}}\left[\exp\left[\frac{-(v-v_0)^2}{2v_t^2}\right] + \exp\left[\frac{-(v+v_0)^2}{2v_t^2}\right]\right], \tag{2}$$

Eq.(1) becomes

$$1 = \frac{\omega_p^2}{4v_t^2k^2}[Z'(\xi_1) + Z'(\xi_2)], \tag{3}$$

where

$$Z(\varsigma) = \frac{1}{\sqrt{\pi}}\frac{\partial}{\partial\varsigma}\int\frac{e^{-x^2}}{x-\varsigma}dx, \tag{4}$$

is the plasma dispersion function [3]. The arguments ξ_1 and ξ_2 are defined by

$$\xi_1 = \frac{1}{v_t\sqrt{2}}(\xi - v_0)$$

and

$$\xi_2 = \frac{1}{v_t\sqrt{2}}(\xi + v_0).$$

There are in general four solutions $\omega(k)$ of the dispersion relation, given real k, $(\pm\omega_{r_1} + \imath\omega_{i_1})$ and $(\pm\omega_{r_2} + \imath\omega_{i_2})$. These were found numerically using Muller's method, and one of each pair appears in Figure 1 for the example $v_t = 0.0$. For small enough k, one pair of roots has a positive imaginary part; this is the growth rate of the mode k. Figure 2 shows this root for several values of v_t. The fastest growth rate , the mode number of the fastest growing mode and the mode number at which the growth rate goes through zero are plotted against v_t in Figure 3.

The Penrose condition gives an independent determination of the value of v_t above which the two stream distribution is stable and below which it is unstable. The Penrose condition is that

$$\int \frac{f(v) - f(\varsigma)}{(v-\varsigma)^2} dv > 0 \tag{5}$$

for stability [4], where $f(\varsigma)$ is a local minimum in the distribution function, $f(v)$, normalized to

$$\int f(v)dv = N.$$

For the two stream distribution (Eq.(2)) the local minimum is at $\varsigma = 0$. A numerical computation using Simpson's rule showed the integral in Eq.(5) to be positive for $v_t \geq 0.77v_0$. Thus the two stream distribution,$F(v)$, is stable if $v_t \geq 0.77v_0$, and is unstable otherwise. The solutions of the dispersion relation,$\omega(k)$ (Eq.(3)),are consistent with this result;$\omega(k)$ shows no growing modes for $v_t \geq 0.77v_0$, but does show growing modes for $v_t < 0.77v_0$.

Simulation

$ES1$ is a one dimensional, electrostatic particle simulation code developed by A. Bruce Langdon[5]. Given the initial positions and velocities of a set of charged particles, $ES1$ solves for the electric fields on grid points (in this case, 128) and uses the fields to compute new particle positions and velocities. This procedure is repeated each time step. The code uses periodic boundary conditions; that is, if a particle leaves one end of the system it will reenter with the same velocity at the other end. The length of the system used is

$$l = \frac{20\pi v_0}{\omega_p},$$

and the time increment is

$$dt = \frac{0.2}{\omega_p}.$$

Input parameters instruct $ES1$ to load the particles (typically 8192) into two beams and within each beam to distribute the velocities in a Maxwellian according to the thermal velocity specified.

Linear Results

Logrithmic plots showing the growth of electrostatic field energy in the various modes are generated by the simulation. Figure 4 contains such plots for rapidly growing modes for several values of v_t. The theoretical growth rates have been sketched in for comparison. The linear nature of the growth is apparent in the cold cases, and agrees with the theoretical predictions.

In the warmer cases, an additional effect makes such a comparison more difficult. There seems to be an additional contribution to the growth of the electrostatic energy which grows nonlinearly and with a much greater level of high frequency oscillations than seen in the cold cases.The effect becomes more and more dominant as the value of v_t is increased. It has been suggested that because there is an increasing difference in velocity between the individual particles in the tail of the Maxwellian as the temperature is increased, perhaps an increasing level of multibeaming between these tail particles is being observed[6]. Two experiments were conducted to test this hypothesis. The number of particles was increased in order to reduce the velocity spread between particles in the tail of the distribution, resulting in a drop in the level of the high frequency, nonlinear contribution to the electrostatic energy. Another test was to observe the evolution of the electrostatic energy of a single nondrifting Maxwellian. The energy did grow in this case, and the growth looked

very similar to the corresponding (same v_t) two stream case. For large values of v_t, the multibeaming instability between the particles in the tail of the distribution may make a larger contribution to the field energy than the two stream instability of the two primary beams. This undesired contribution to the field enery can be reduced by increasing the number of particles in the simulation (see Figure 5), but for practical numbers of particles the effect still obscures the linear growth for some values of v_t. This study did not go deeper into resolving the multibeaming problem.

Nonlinear Results

As the system evolves in time, depending on the initial temperature, the two streams may remain distinct, or particle mixing may take place until the original beams are no longer distinguishable. In the cold case the instability is severe, and the two stream character is lost. Figure 6a shows plots of the total distribution function, $f(v)$, for $v_t = 0$ at intervals of twenty time steps. Figure 6b shows plots of the distribution of velocities of the particles from just one of the original beams at the same time intervals. After the seventh plot in Figure 6b, the mean velocity has decreased to zero from its initial value $v_0 = 1$. For the very warm example in Figure 7 ($v_t = 0.7v_0$, still unstable by the Penrose criterion) the instability has only a minor effect on the distribution and the two stream character is retained.

In some of the intermediate cases an additional phenomenon occurs. The results of a simulation for $v_t = 0.1$ are shown in Figure 8. The total distribution oscillates between a double peaked and single peaked curve centered at $v = 0$. This is due to the spiralling of the streams in phase space as seen in the sequence of Figure 9. Eventually, the instability saturates, oscillation is no longer observed and the distribution function $f(v)$ is left with a single hump.

In order to study the final state quantitatively, a single parameter is introduced which indicates the form of the distribution function. Specifically, N_0, the number of particles with velocity equal to zero (in practice, the number of particles with velocity in the range $-\Delta u < v < \Delta u$, where $\Delta u \ll v_0$) gives a measure of the size of the dip in the distribution function at $v = 0$ and thus a measure of the extent to which the two streams have remained distinct. Given the total number of particles and the total kinetic energy in the system, a single Maxwellian centered at $v = 0$ can be completely specified, and N_0 for this theoretical limit can be computed from the simulation parameters, and is called N_0m. These two parameters (total number of particles and kinetic energy) were also used to determine a two stream distribution with peaks at $v = \pm 1$. which is marginally stable by the Penrose criterion, allowing a theoretical estimate of N_0 for marginal stability, called N_0p.

If the instability completely randomized the particle positions in phase space, the expected final distribution of velocities would be a single Maxwellian centered at $v = 0$. Since a single Maxwellian has no dip at $v = 0.$, this randomization would result in an upper limit on the value of N_0. Alternatively, if the instability saturated at the point of marginal stability, a minimum value of N_0 would result. The values of N_0 found in the simulations have been compared with these two limits.

Assuming that the form of the distribution function in the saturation state is bimaxwellian, then the Penrose condition for marginal stability is $v_{tp} = 0.77v_{0p}$, where v_{tp} is the thermal velocity associated with the two beams. Then N_0 for the Penrose stable case (N_{0p}) is

$$N_{0p} = \frac{2\Delta uN}{\sqrt{\pi K/m}} e^{-\frac{1}{2}(\frac{1}{0.77})^2}, \tag{6}$$

and for the single Maxwellian,

$$N_{0m} = \frac{2\Delta u N}{\sqrt{\pi K/m}}. \tag{7}$$

(K is the average kinetic energy per particle, and N is the number of particles per beam.)

Plots of N_0 vs. time for various initial temperatures are shown in figure 10. The values of N_{0p} and N_{0m} have been sketched in for comparison. As expected, N_0 decreases with respect to the theoretical values as the beams are warmed. In the colder cases, it is somewhere between the two extremes, and in the warmer cases it is near N_{0p}. The large oscillations seen in N_0, particularly for $v_t = 0.1$, are due to the spiralling of the streams in phase space as described previously.

Conclusion

The dispersion relation for the instability changed smoothly as the thermal velocity was increased. The growth rates from the simulations agreed with the theoretical values, to the extent to which they could be obtained. The final shape of $f(v)$ varied gradually with v_t from a single peaked distribution for the cold case to an almost unchanged double peaked distribution in the warm case. No sudden transitions were observed; i. e., there appears to be no special value of v_t/v_0.

APPENDIX A- Calculation of N_{0m}, the number of particles with velocities in the range $-\Delta u < v < \Delta u$ for a single Maxwellian centered on $v = 0$ with the same total number of particles and total kinetic energy as the initial two stream distribution used in the particle simulations.

In order to compute N_{0m}, it is necessary to compute the root mean square velocity, v_m of the particles in the single Maxwellian. v_m can be found by equating the total energy of the particles in the single Maxwellian to the total particle energy in the two stream distribution:

$$\frac{1}{2}(2N)mv_m^2 = \frac{1}{2}(2N)m(v_0^2 + v_t^2). \tag{8}$$

Thus,

$$v_m^2 = v_0^2 + v_t^2. \tag{9}$$

The normalization for the distribution is found by integrating over velocities to get the total number of particles:

$$\int_{-\infty}^{\infty} A \exp\Big[\frac{-v^2}{2v_m^2}\Big] dv = 2N. \tag{10}$$

N is the number of particles in each beam. The normalization constant is:

$$A = \frac{N}{v_m}\sqrt{\frac{2}{\pi}}. \tag{11}$$

By integrating the normalized distribution function between $-\Delta u$ and Δu, the number of particles with velocity between these limits can be computed:

$$N_{0m} = \frac{N}{v_m}\sqrt{\frac{2}{\pi}} \int_{-\Delta u}^{\Delta u} \exp\Big[\frac{-v^2}{2v_m^2}\Big] dv. \tag{12}$$

Since $\Delta u \ll v_0$, the integral may be approximated by multiplying the length of the interval,$2\Delta u$, by the value of the integrand evaluated at $v = 0.$, resulting in the final expression

$$N_{0m} \simeq \frac{2\Delta u N}{v_m}\sqrt{\frac{2}{\pi}}. \tag{13}$$

The average kinetic energy per particle is thus

$$K = \frac{1}{2}mv_m^2.$$

APPENDIX B- Calculation of N_{0p}, the number of particles with velocities in the range $-\Delta u < v < \Delta u$ for a bimaxwellian centered on $v = 0$ with $v_t = 0.77$ and with the same total number of particles and total kinetic energy as the initial two stream distribution used in the particle simulations.

This calculation is analogous to that for N_{0m}. The total energy of the particles in a marginally Penrose stable bimaxwellian is

$$NK = \frac{1}{2}m\left(2N\right)\left(v_{tp}^2 + v_{0p}^2\right)$$

where K is again the average kinetic energy per particle, v_{0p} is the beam velocity and v_{tp} is the thermal velocity. For the marginally stable case, $v_{tp} = 0.77v_{0p}$. Equating this energy to the total energy given of the particles in the simulations,

$$\frac{1}{2}m\left(2N\right)\left(v_{tp}^2 + v_{0p}^2\right) = \frac{1}{2}m\left(2N\right)\left(v_0^2 + v_t^2\right).$$

Thus,

$$v_{0p}^2 = \frac{v_0^2 + v_t^2}{\left(1. + (0.77)^2\right)} = \frac{v_0^2 + v_t^2}{1.593}.$$

The appropriate Penrose stable distribution is thus

$$f_p(u) = B\left(\exp\left[-\frac{(u-v_{0p})^2}{2v_{tp}^2}\right] + \exp\left[-\frac{(u+v_{0p})^2}{2v_{tp}^2}\right]\right).$$

Normalizing to find the constant B,

$$\int_{-\infty}^{\infty} f_p(u)du = 2N$$

gives

$$B = \frac{N}{v_{tp}\sqrt{2\pi}}.$$

Integrate $f_p(u)$ between $-\Delta u$ and Δu to find N_{0p}:

$$N_{0p} = \frac{N}{v_{tp}\sqrt{2\pi}}\int_{-\Delta u}^{\Delta u}\left(\exp\left[-\frac{(u-v_{0p})^2}{2v_{tp}^2}\right] + \exp\left[-\frac{(u+v_{0p})^2}{2v_{tp}^2}\right]\right)du,$$

or

$$N_{0p} \simeq \frac{2\Delta uN}{v_{tp}\sqrt{2\pi}}\exp\left[-\frac{v_{0p}^2}{2v_{tp}^2}\right] = 0.43\frac{2\Delta uN}{\sqrt{\pi K/m}}.$$

Acknowledgments

I thank Professor C. K. Birdsall for his help with this project. Research sponsored by the Office of Naval Research Contract N00014-77-C-0578. Simulations were done on NMFECC at LLNL, Livermore.

References

[1] S. Kainer, J. Dawson and R. Shanny. Phys. Fluids 15,493 (1971).

[2] N. Krall and A. Trivelpiece. Principles Of Plasma Physics, p.374 (1973).

[3] B. D. Fried and S. Conte, The Plasma Dispersion Function, Academic (New York,1961).

[4] Krall, op. cit., p.470.

[5] C. K. Birdsall and A. B. Langdon. Plasma Physics via Computer Simulation, McGraw-Hill (New York,1985).

[6] Ibid., p.394.

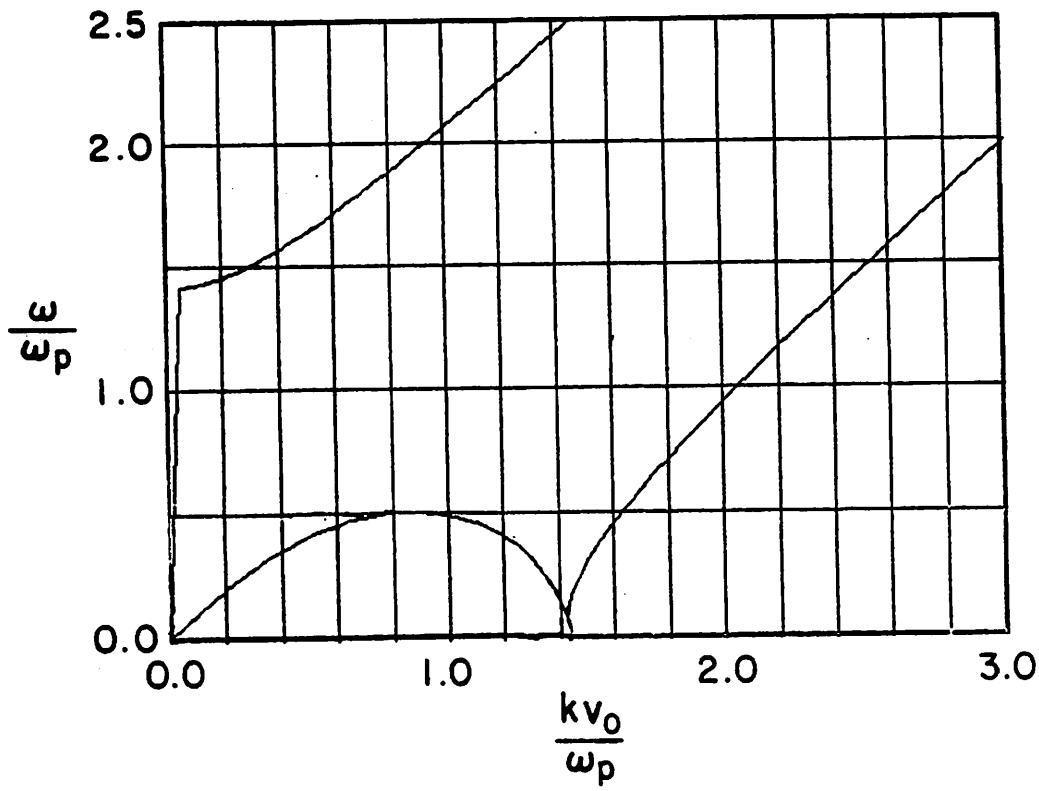

Figure 1: Dispersion relation for $v_t/v_0 = 0.0$. The curve which intersects the $\omega = 0.$ axis twice is ω_i. The other two are ω_r. For $\frac{kv_0}{\omega_p} > 1.41$, ω_i is 0.

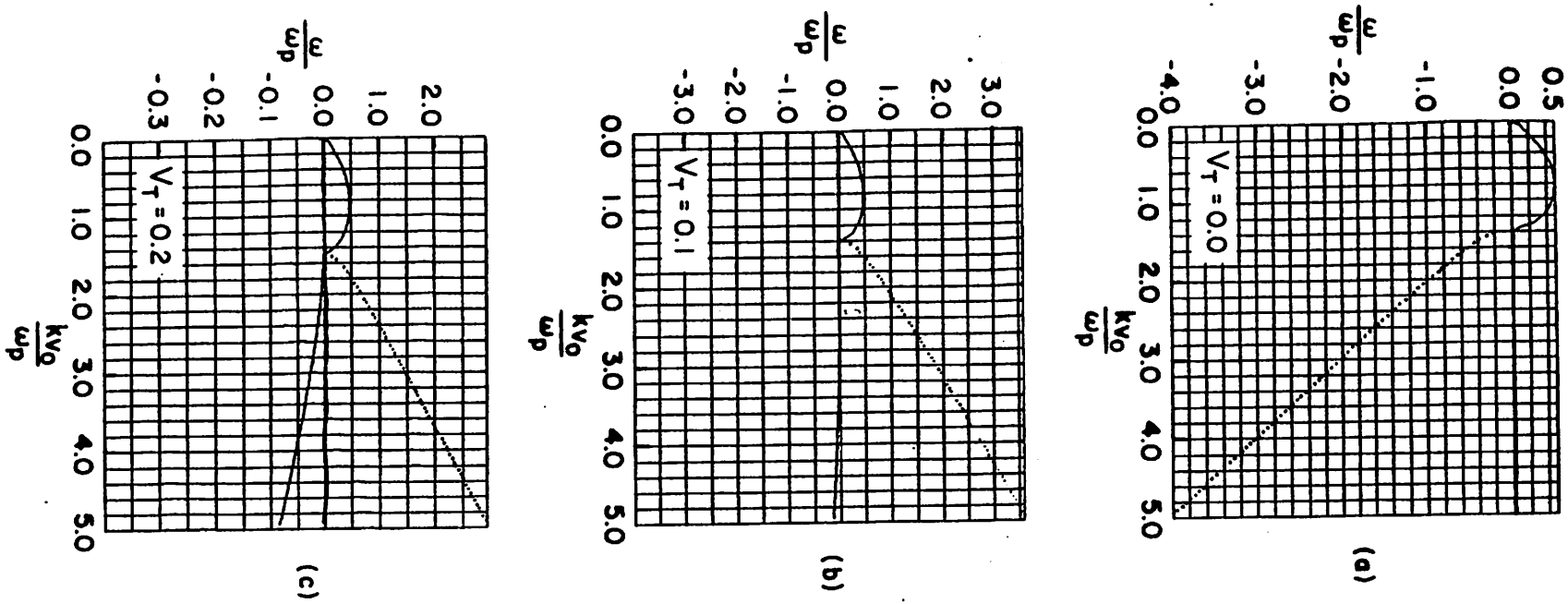

Figure 2: Dispersion relation for successive values of v_t/v_0. The solid line represents the imaginary part of the frequency, ω_i/ω_p,and the dotted line represents the real part ω_r/ω_p. Only one of the two branches $\pm\omega_r/\omega_p$ was followed by the root solver. The negative root is shown in (a), (d), (e) and (f), and the positive root is shown in (b) and (c). Note that both positive and negative roots exist for all cases, but that only one root was plotted.

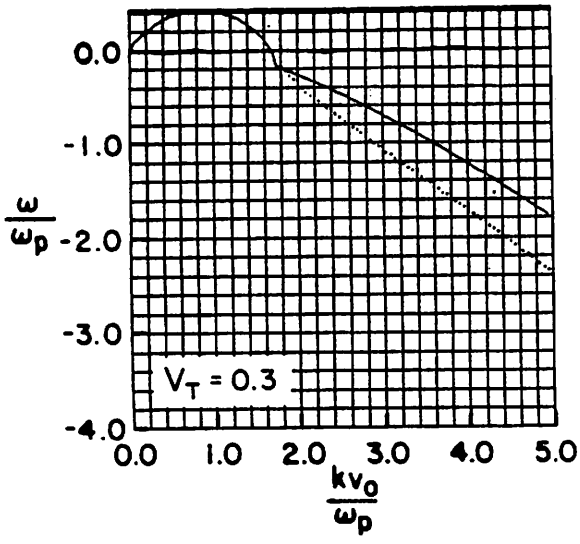
0.0
-1.0
-2.0
-3.0
-4.0
$\frac{\omega}{\omega_p}$
$V_T = 0.3$
0.0 1.0 2.0 3.0 4.0 5.0
$\frac{kv_0}{\omega_p}$

(d)

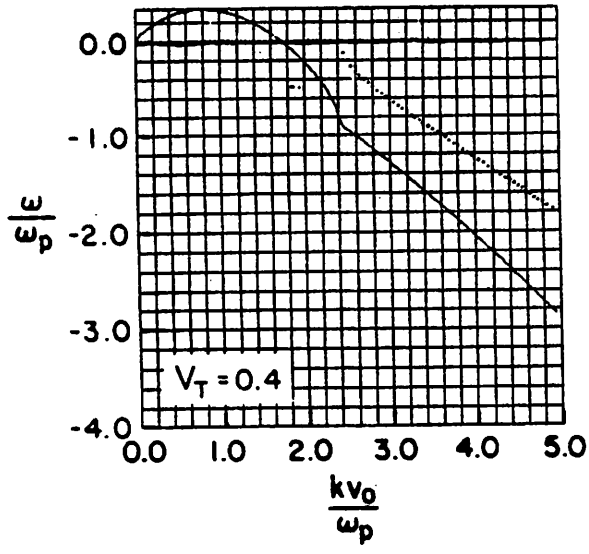
0.0
-1.0
-2.0
-3.0
-4.0
$\frac{\omega}{\omega_p}$
$V_T = 0.4$
0.0 1.0 2.0 3.0 4.0 5.0
$\frac{kv_0}{\omega_p}$

(e)

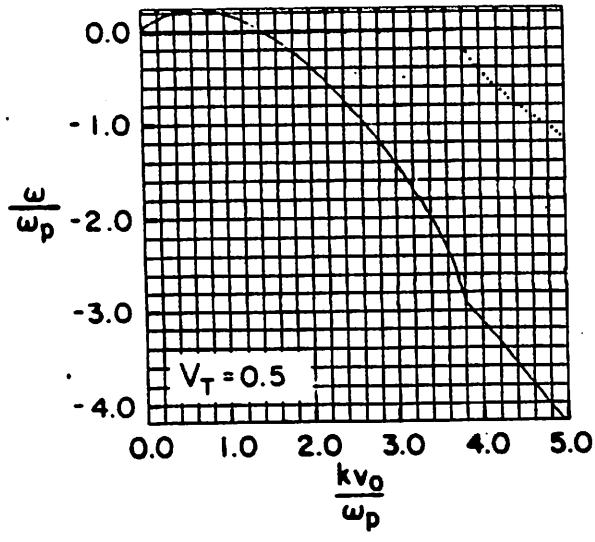
0.0
-1.0
-2.0
-3.0
-4.0
$\frac{\omega}{\omega_p}$
$V_T = 0.5$
0.0 1.0 2.0 3.0 4.0 5.0
$\frac{kv_0}{\omega_p}$

(f)

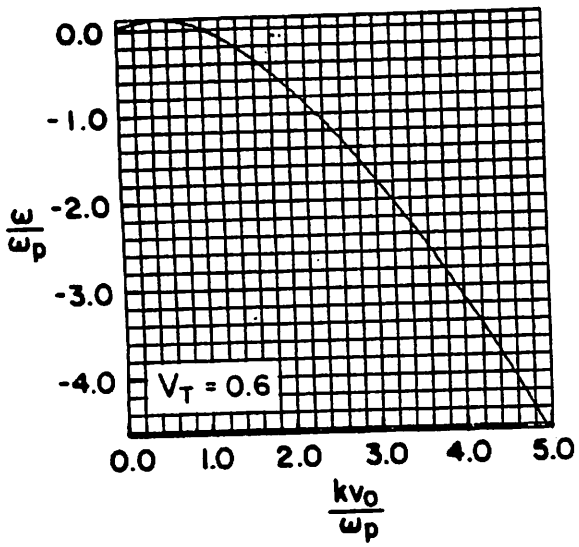
0.0
-1.0
-2.0
-3.0
-4.0
$\frac{\omega}{\omega_p}$
$V_T = 0.6$
0.0 1.0 2.0 3.0 4.0 5.0
$\frac{kv_0}{\omega_p}$

(g)

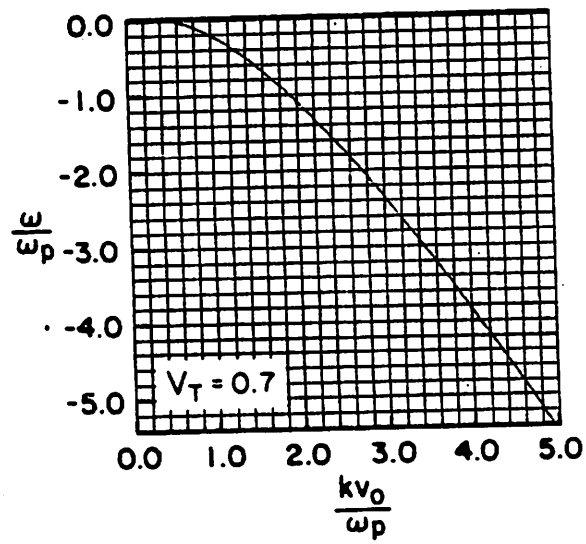
0.0
-1.0
-2.0
$\frac{\omega}{\omega_p}$ -3.0
-4.0
-5.0
$V_T = 0.7$
0.0 1.0 2.0 3.0 4.0 5.0
$\frac{kv_0}{\omega_p}$

(h)

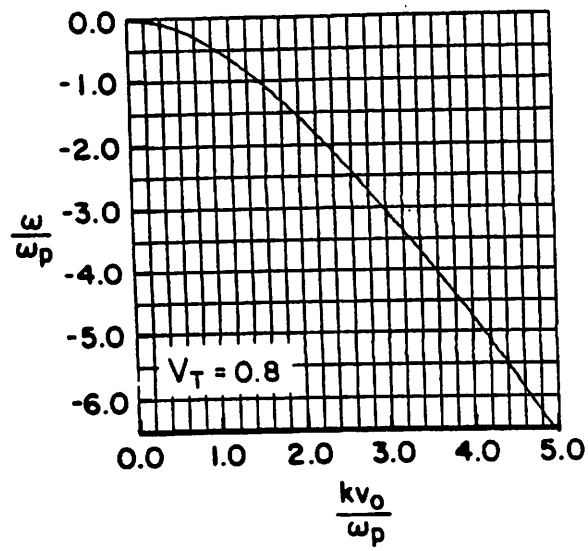
0.0
-1.0
-2.0
$\frac{\omega}{\omega_p}$ -3.0
-4.0
-5.0
-6.0
$V_T = 0.8$
0.0 1.0 2.0 3.0 4.0 5.0
$\frac{kv_0}{\omega_p}$

(i)

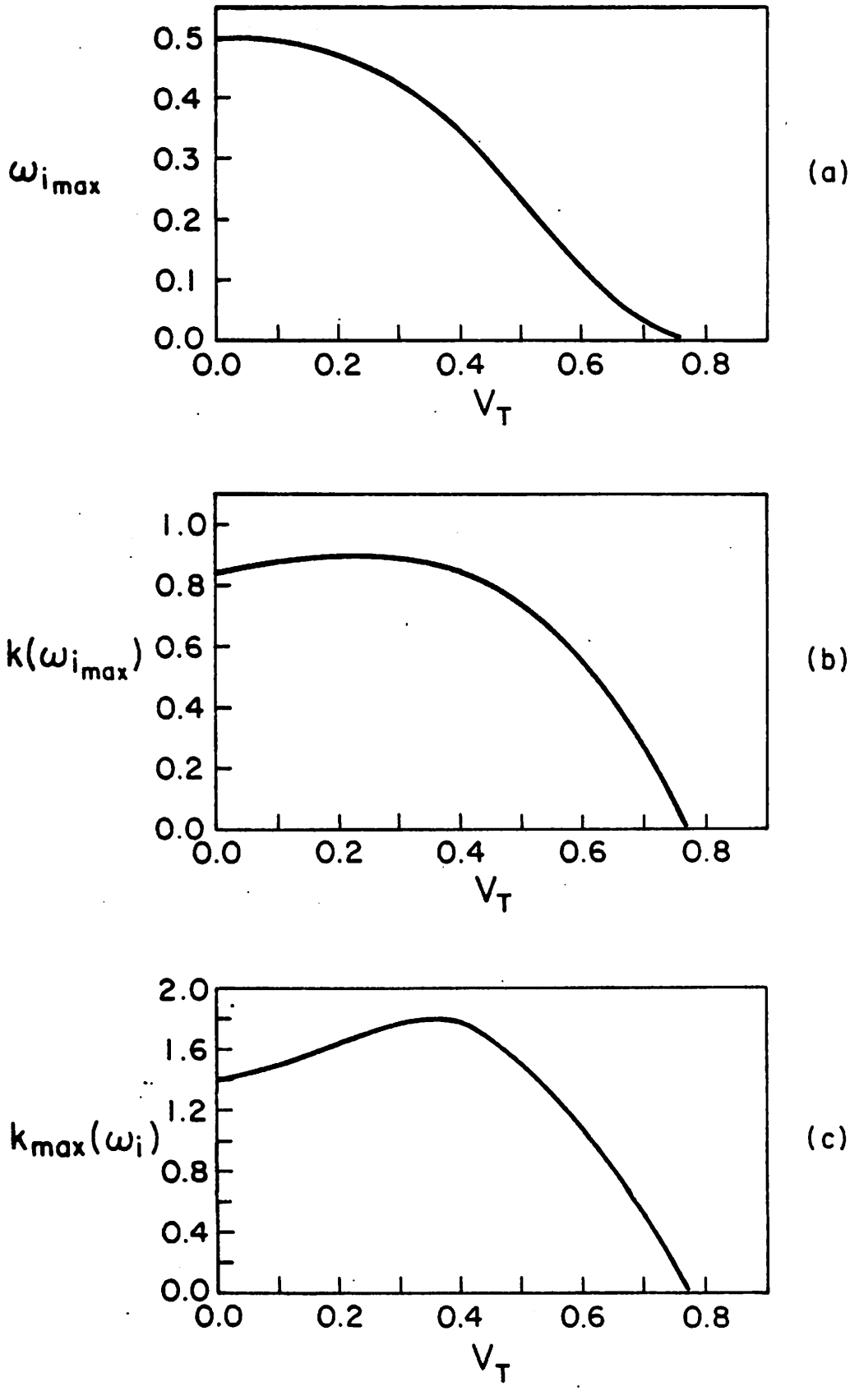

Figure 3: Dispersion relation numerical solutions: plots of (a) maximum growth rate vs. thermal velocity of beams, (b) wave number of fastest growing mode vs. thermal velocity, and (c) the mode number at which the growth rate goes through zero vs. the thermal velocity. ω_i is normalized to ω_p, k is normalized to v_0/ω_p and v_t is normalized to v_0.

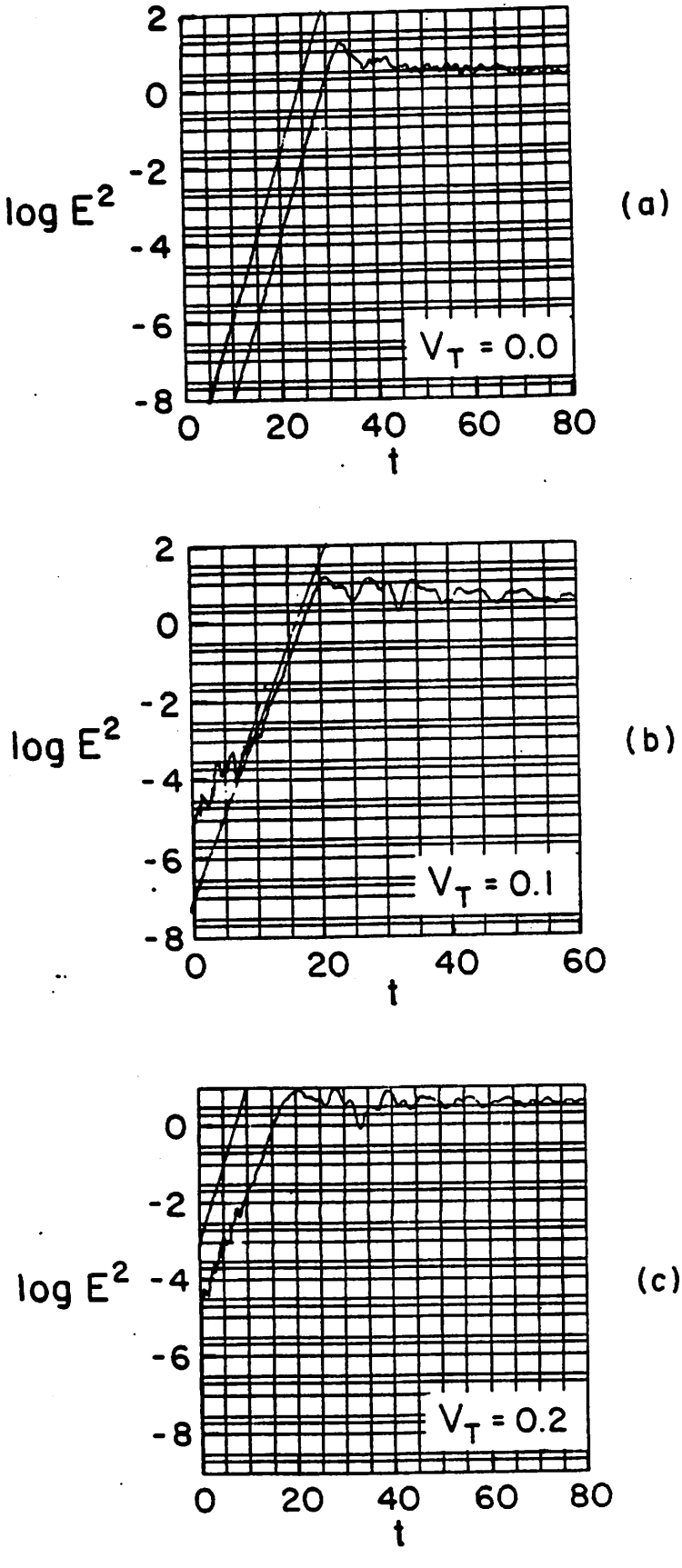

Figure 4: Field energy vs. time for various values of v_t, with 4096 particles per beam. Note higher frequency oscillations early in time, progressively more pronounced for increasing v_t. This is possibly a numerical aberration due to a multibeaming instability between particles in the tail of the distribution function. The straight lines which have been drawn in show the growth rate of the fastest growing mode given by the solution of the dispersion relation.

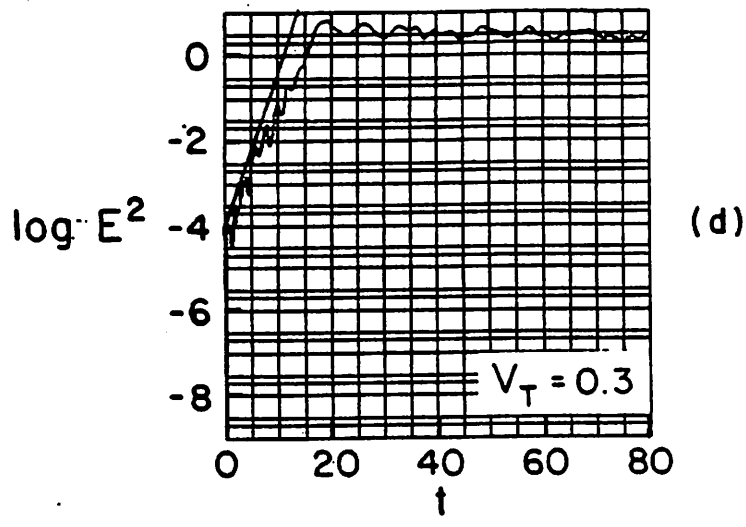
log E²
0
-2
-4
-6
-8
V_T = 0.3
0
20
40
60
80
t

(d)

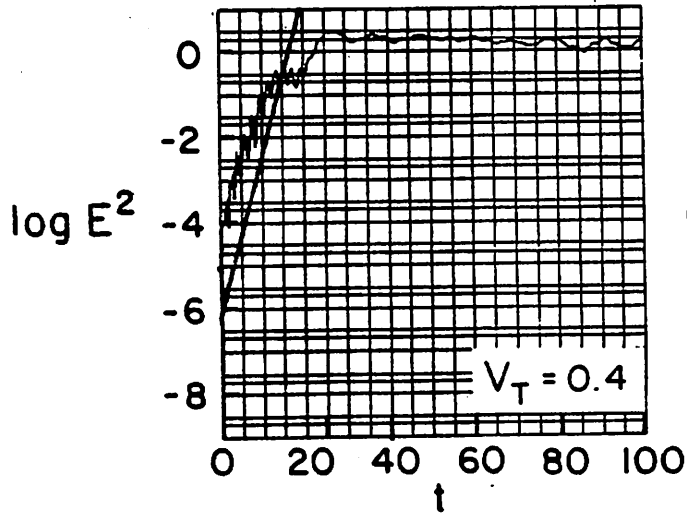
log E²
0
-2
-4
-6
-8
V_T = 0.4
0
20
40
60
80
100
t

(e)

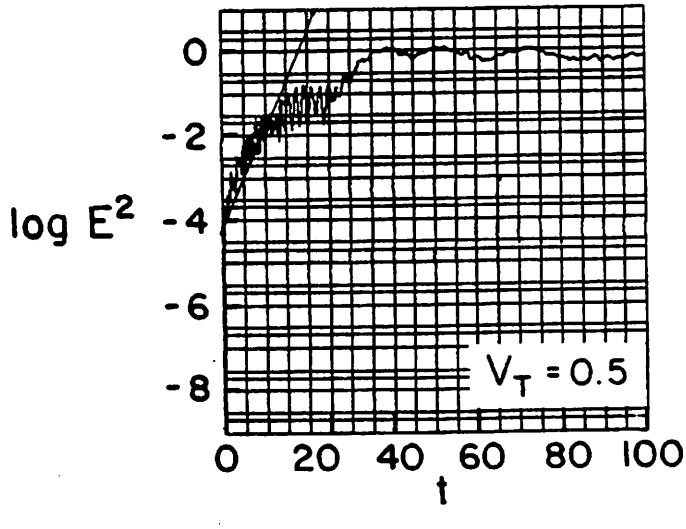
log E²
0
-2
-4
-6
-8
V_T = 0.5
0
20
40
60
80
100
t

(f)

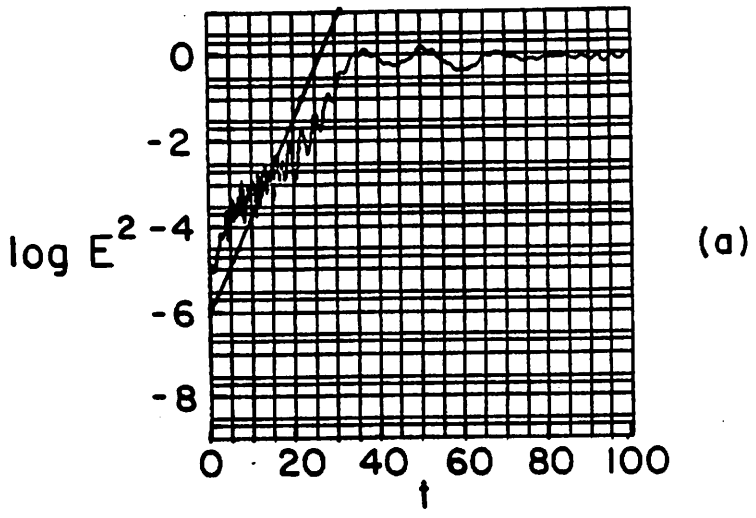

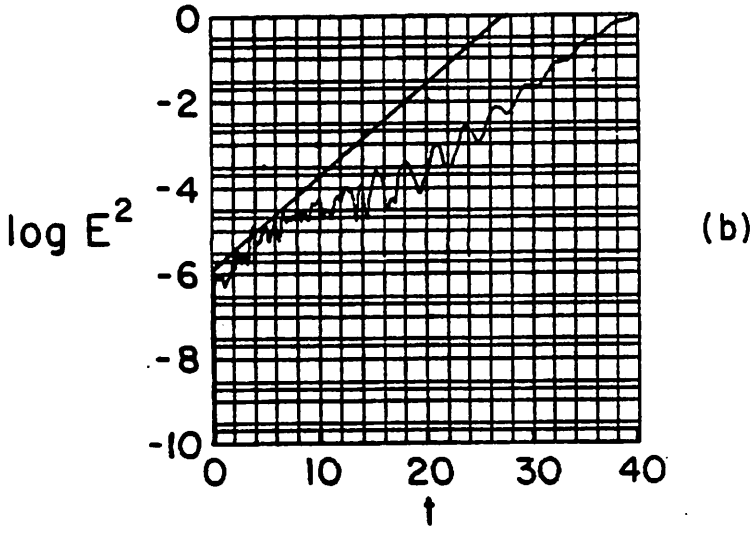

Figure 5: Field energy vs. time for $v_t = 0.5$ for the cases (a) 16384 particles per beam and (b) 65536 particles per beam.

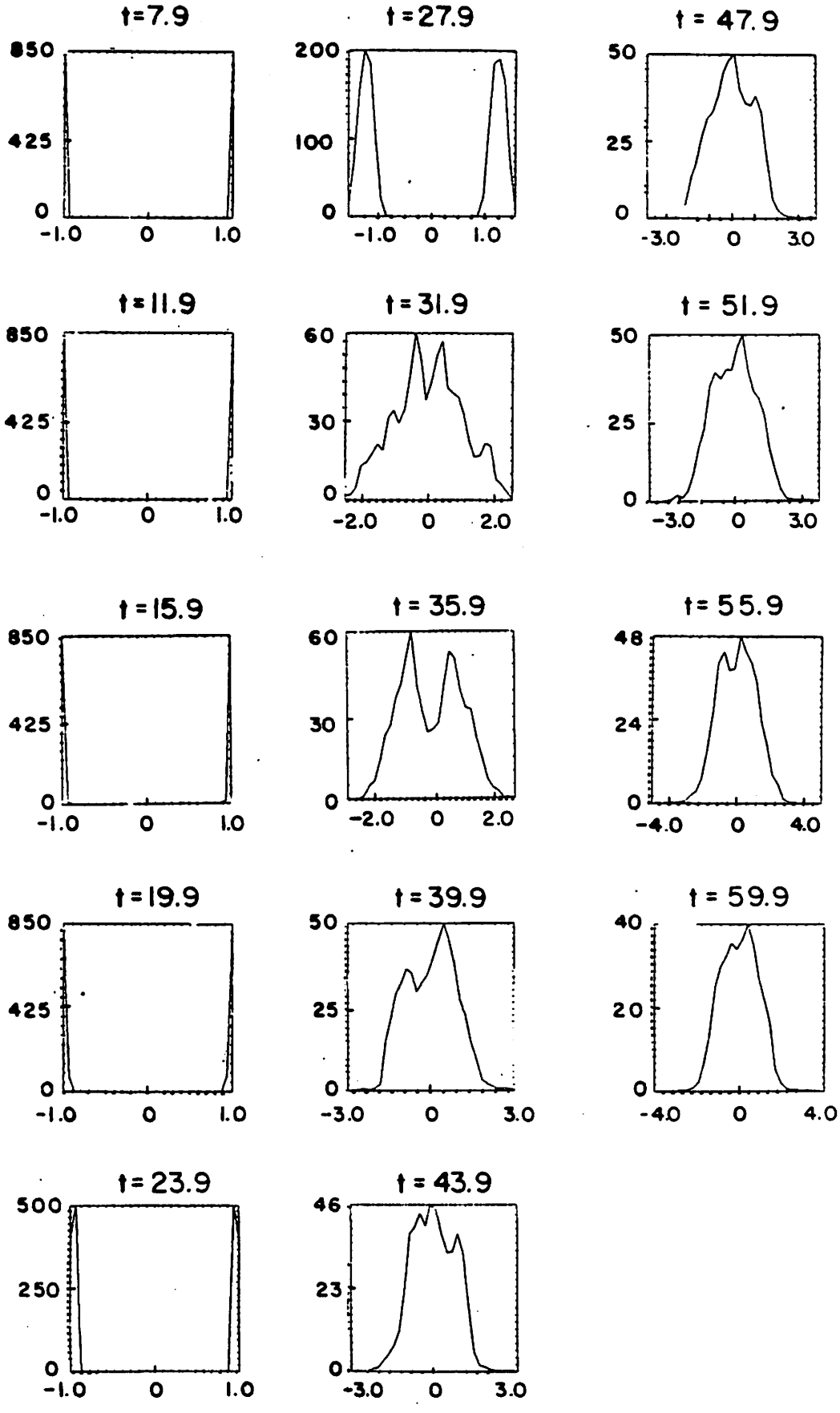

Figure 6: Time evolution of the distribution function, $f(v)$ for $v_t = 0.0$. (a) shows the evolution of the particles in both beams and (b) follows the particles of just one of the original beams.

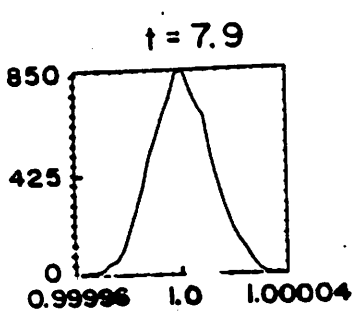
t = 7.9
850
425
0
0.99996
1.0
1.00004

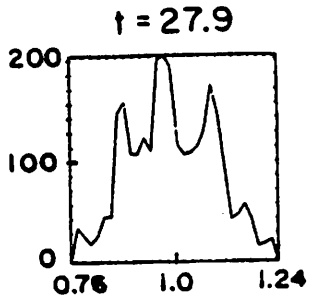
t = 27.9
200
100
0
0.76
1.0
1.24

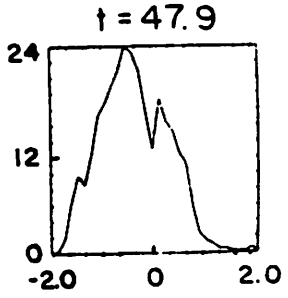
t = 47.9
24
12
0
-2.0
0
2.0

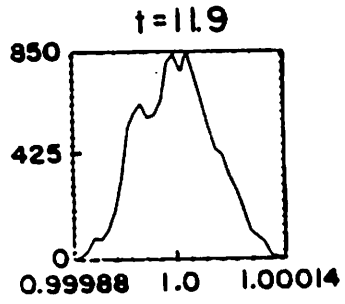
t = 11.9
850
425
0
0.99988
1.0
1.00014

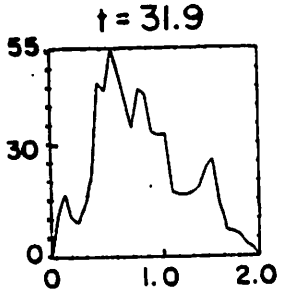
t = 31.9
55
30
0
0
1.0
2.0

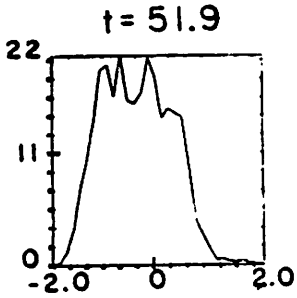
t = 51.9
22
11
0
-2.0
0
2.0

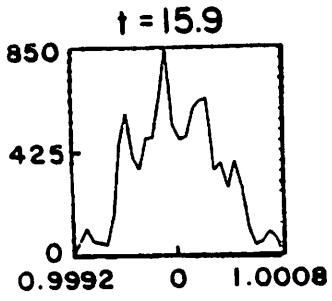
t = 15.9
850
425
0
0.9992
0
1.0008

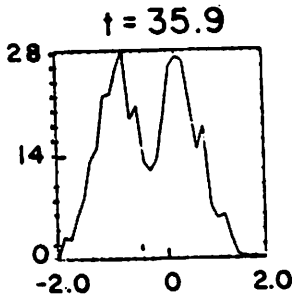
t = 35.9
28
14
0
-2.0
0
2.0

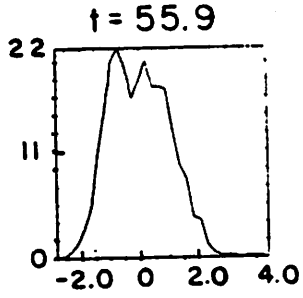
t = 55.9
22
11
0
-2.0
0
2.0
4.0

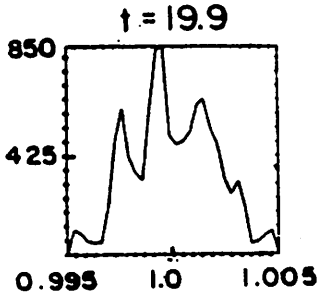
t = 19.9
850
425
0.995
1.0
1.005

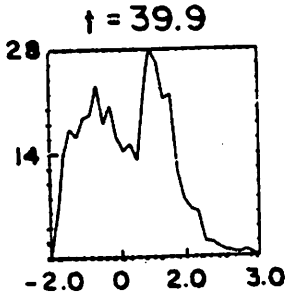
t = 39.9
28
14
-2.0
0
2.0
3.0

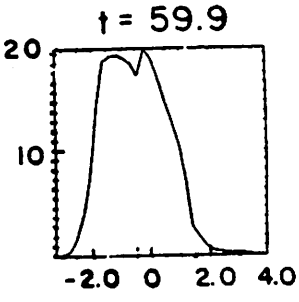
t = 59.9
20
10
-2.0
0
2.0
4.0

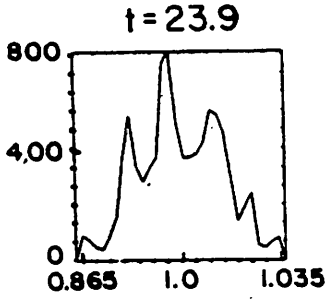
t = 23.9
800
4,00
0
0.865
1.0
1.035

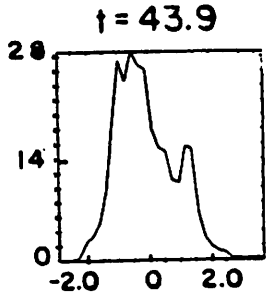
t = 43.9
28
14
0
-2.0
0
2.0

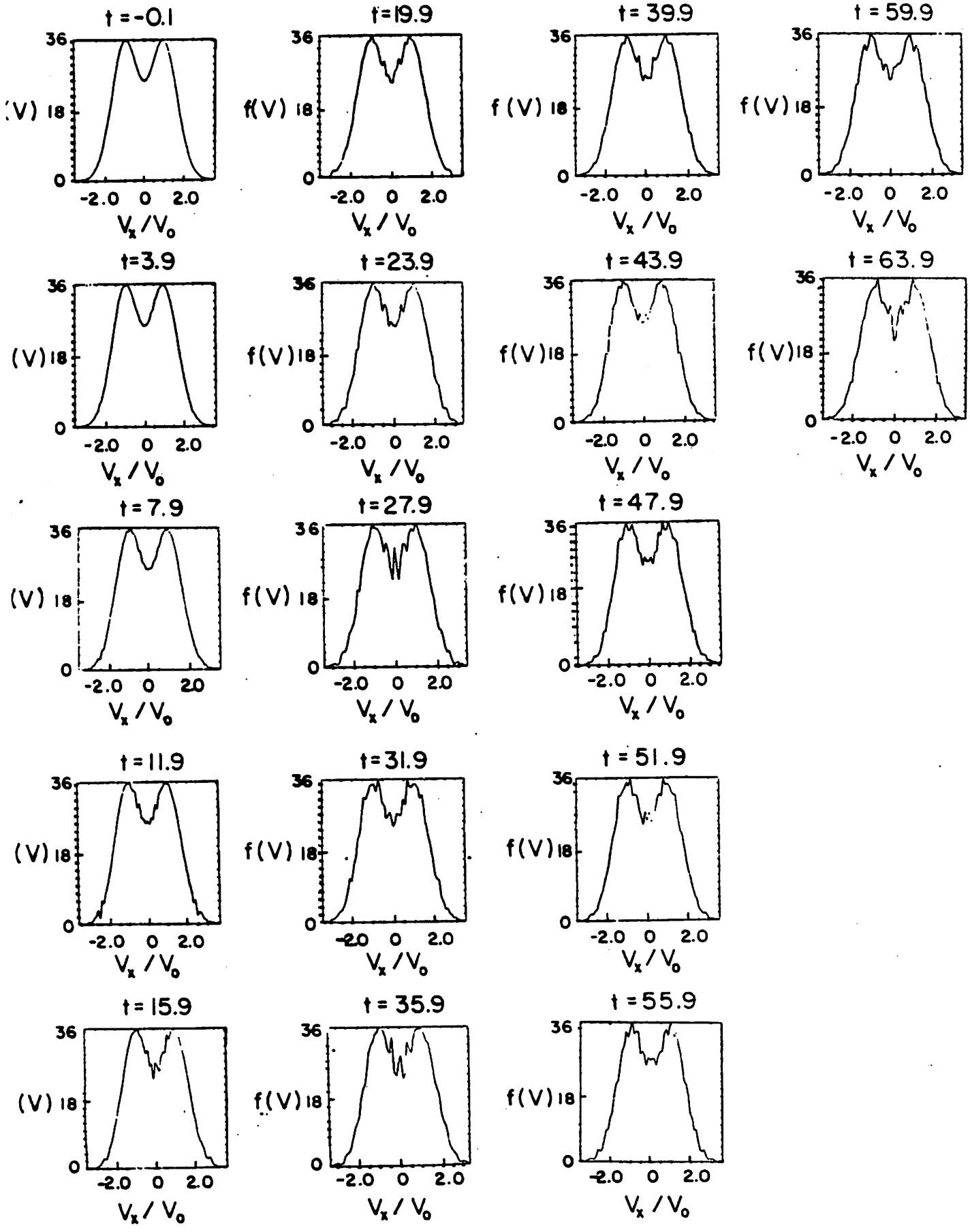

Figure 7: Time evolution of the distribution function, $f(v)$ for $v_t = 0.7$. (a) shows the evolution of the particles in both beams and (b) follows the particles of just one of the original beams.

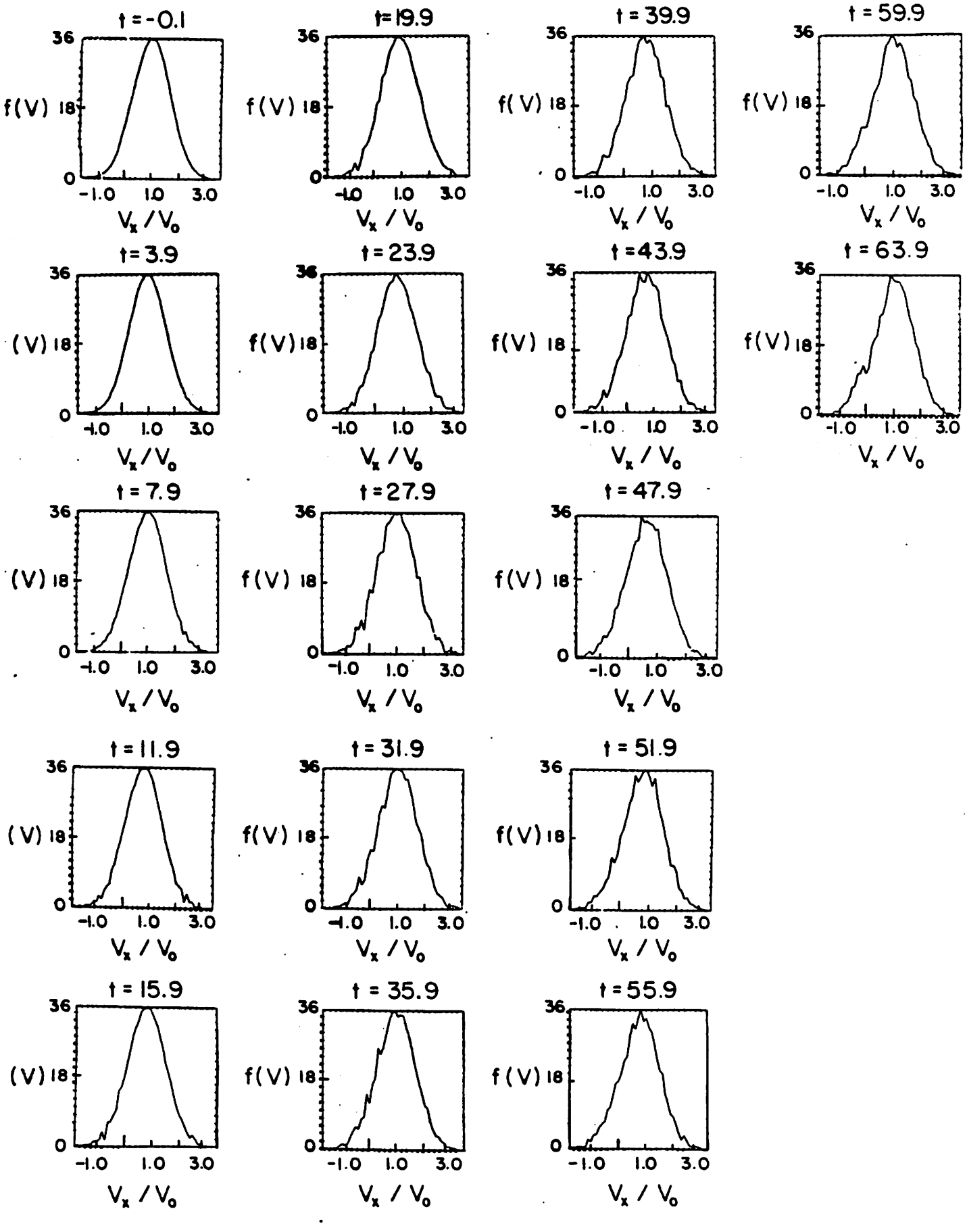
t = -0.1
t = 19.9
t = 39.9
t = 59.9
t = 3.9
t = 23.9
t = 43.9
t = 63.9
t = 7.9
t = 27.9
t = 47.9
t = 11.9
t = 31.9
t = 51.9
t = 15.9
t = 35.9
t = 55.9
f(V)
36
18
0
-1.0
1.0
3.0
V_x / V_0

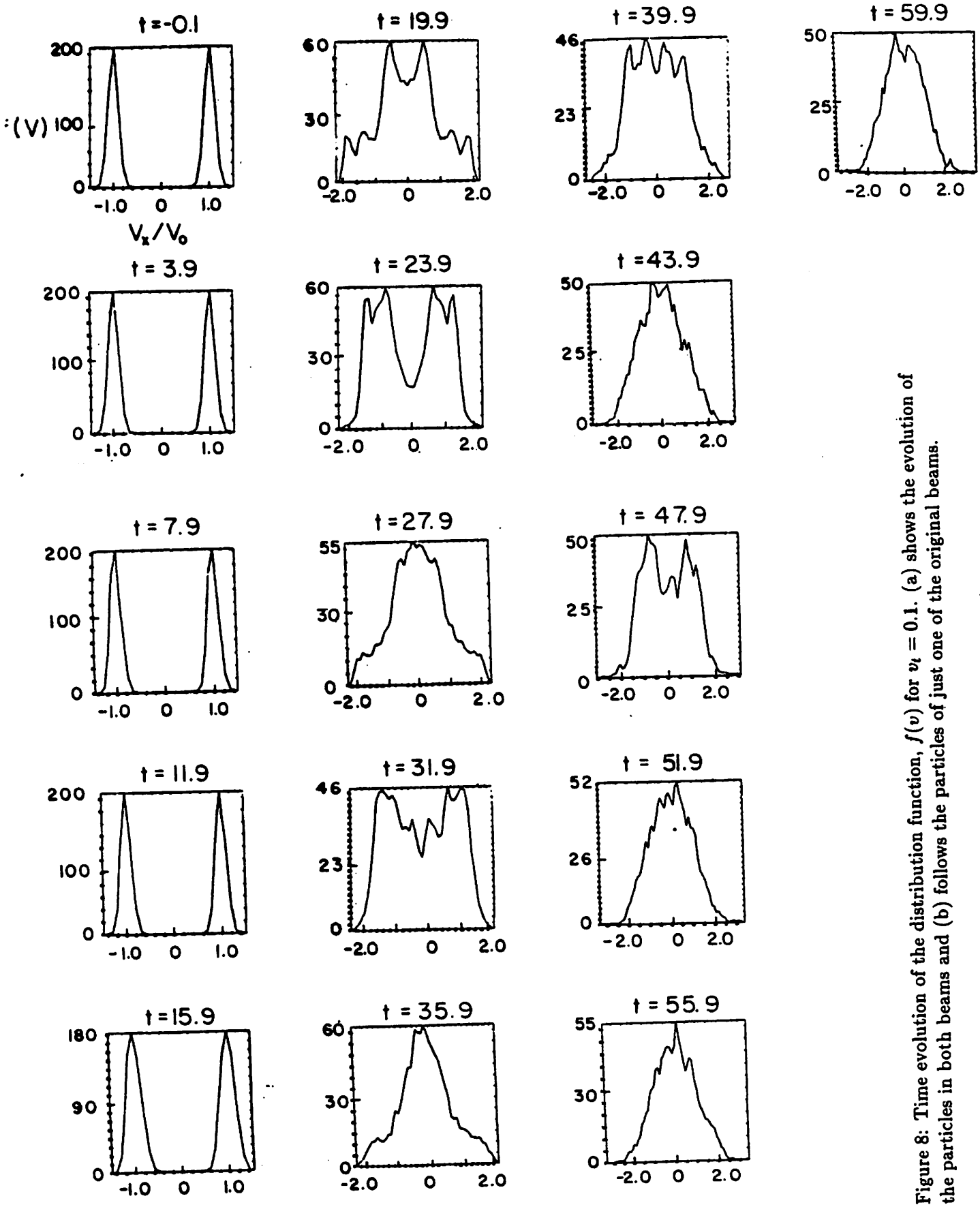

Figure 8: Time evolution of the distribution function, $f(v)$ for $v_t = 0.1$. (a) shows the evolution of the particles in both beams and (b) follows the particles of just one of the original beams.

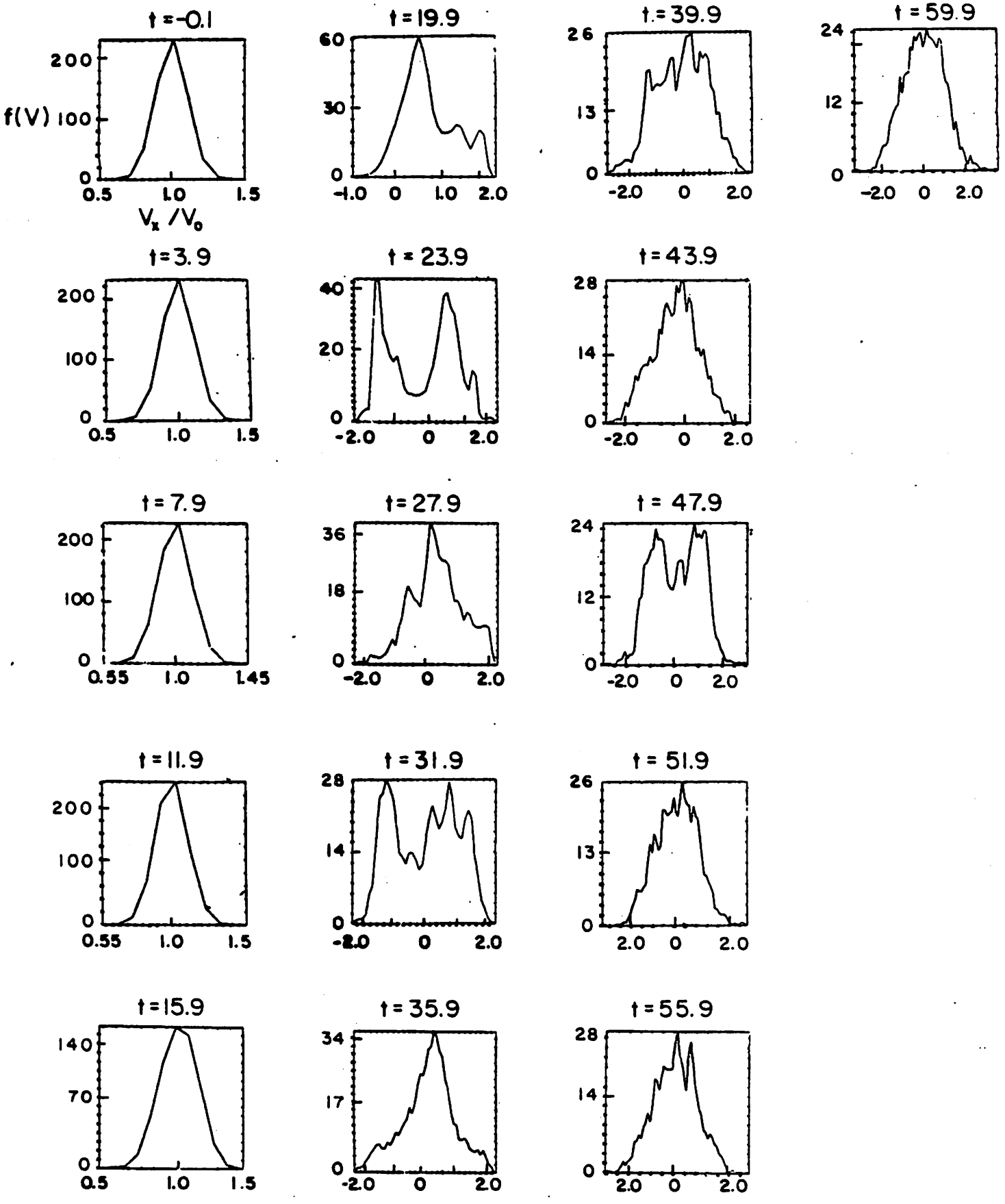
t = -0.1
t = 19.9
t = 39.9
t = 59.9
f(V)
200
100
0
0.5
1.0
1.5
60
30
-1.0
2.0
26
13
-2.0
24
12
V_x / V_0
t = 3.9
t = 23.9
t = 43.9
40
20
28
14
t = 7.9
t = 27.9
t = 47.9
0.55
1.45
36
18
t = 11.9
t = 31.9
t = 51.9
t = 15.9
t = 35.9
t = 55.9
140
70
34
17

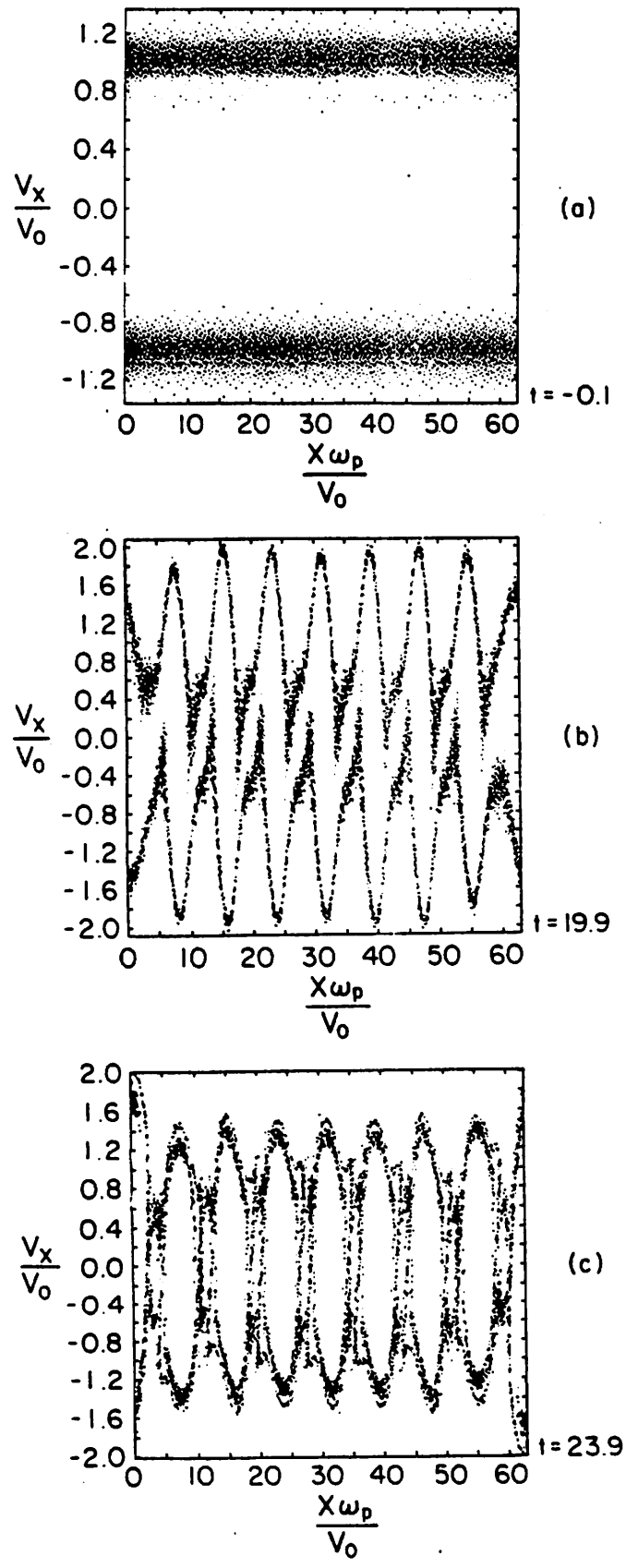

Figure 9: Phase space, v_x/v_0 vs. x/l at times $t = -0.1(0.2/\omega_p)$, $t = 19.9/\omega_p$ and $t = 23.9/\omega_p$ for thermal velocity $v_t = 0.1$. Note that at time $t = 19.9/\omega_p$, the bulk of the particles have near zero velocity.

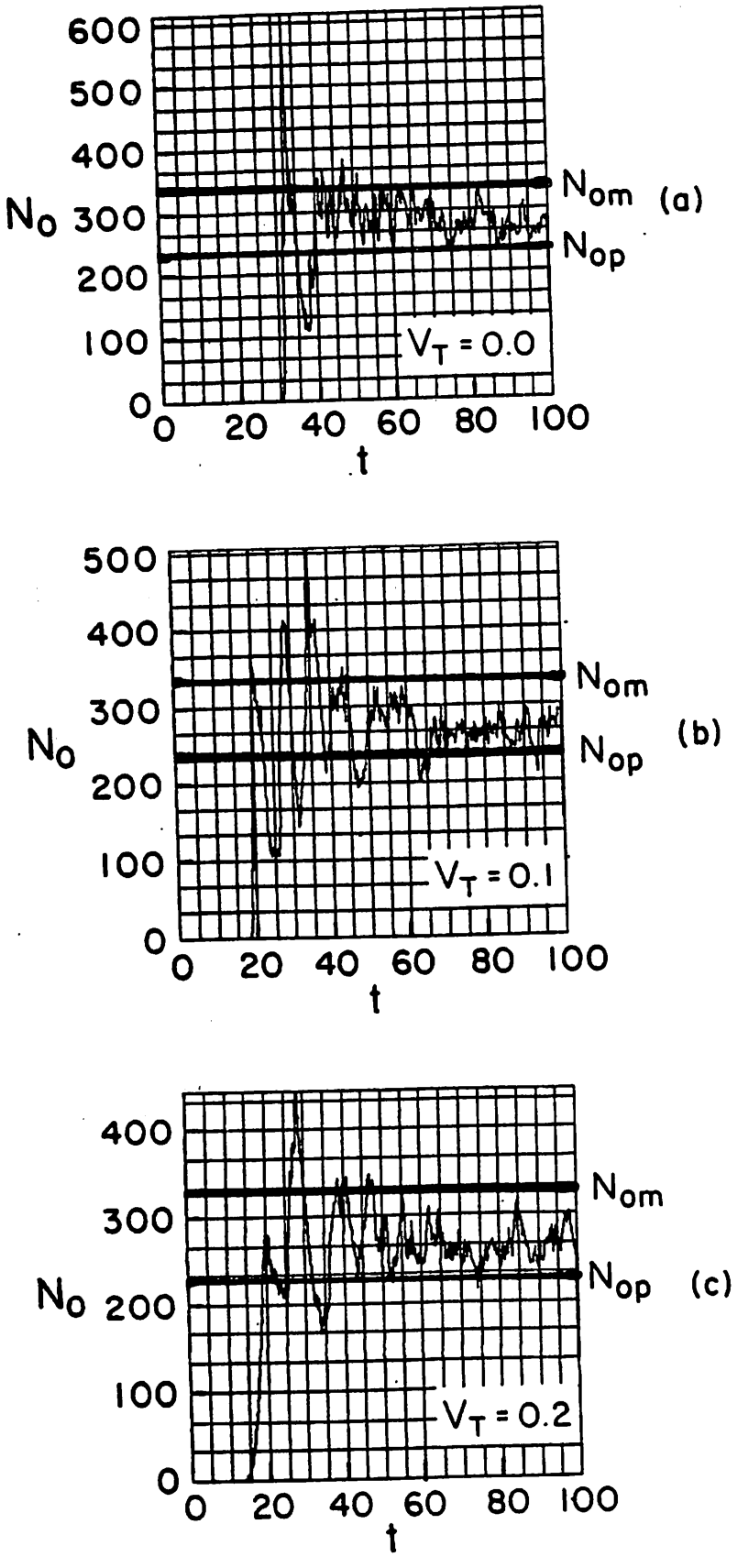

Figure 10:Plots of the number of particles with $|v| \leq 0.05v_0$, N_{0p}, vs. time for various values of v_t. Values of N_{0m} for a Maxwellian with the same number of particles and thermal energy as initially given to the beams in the simulation have been indicated. In addition, N_{0p} for a marginally stable double humped distribution with the same initial parameters is also indicated.

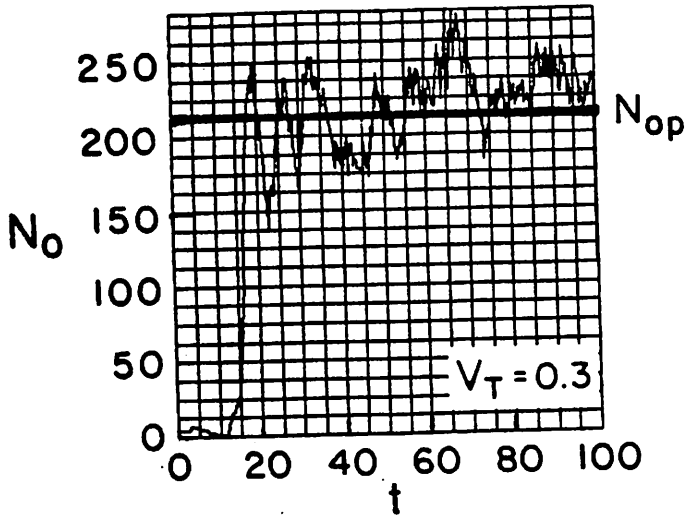
250
200
150
100
50
0
N_0
N_{op}
$V_T = 0.3$
0 20 40 60 80 100
t

(d)

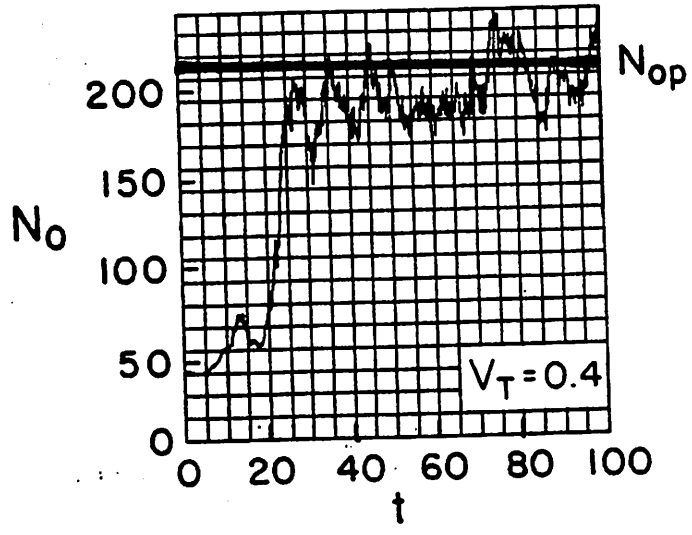
200
150
100
50
0
N_0
N_{op}
$V_T = 0.4$
0 20 40 60 80 100
t

(e)

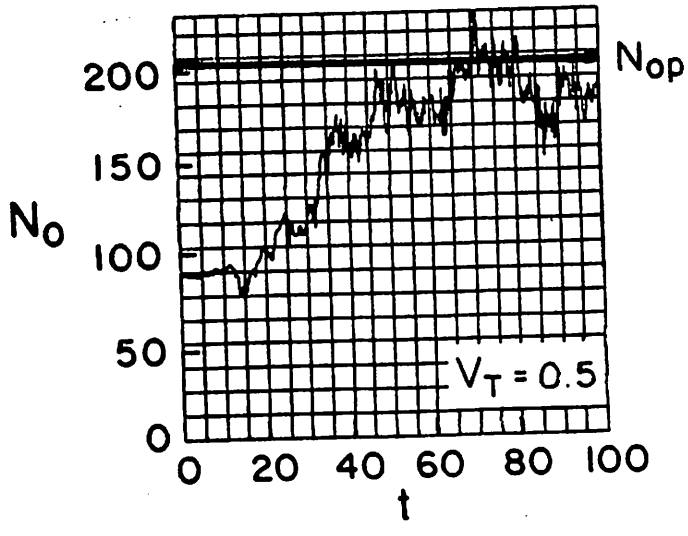
200
150
100
50
0
N_0
N_{op}
$V_T = 0.5$
0 20 40 60 80 100
t

(f)

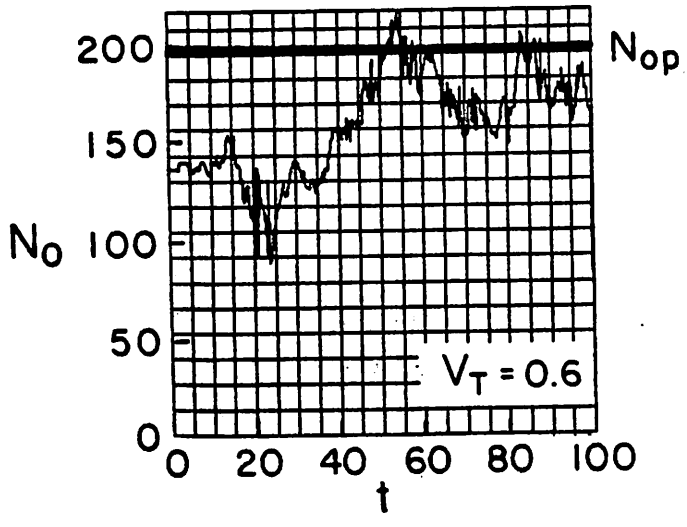
200
150
100
50
0
N_0
N_{op}
$V_T = 0.6$
0 20 40 60 80 100
t

(g)

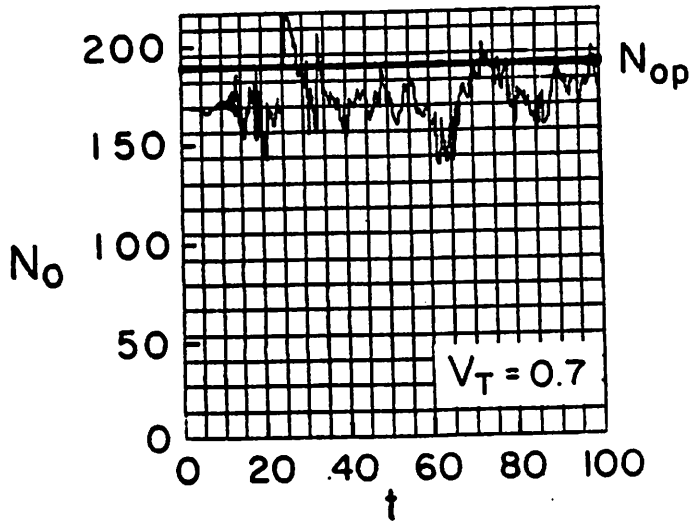
200
150
100
50
0
N_0
N_{op}
$V_T = 0.7$
0 20 40 60 80 100
t

(h)